



Universiteit
Leiden
The Netherlands

Discovery of small molecules inhibitors of EphA4

Farenc, C.

Citation

Farenc, C. (2012, September 13). *Discovery of small molecules inhibitors of EphA4*. Retrieved from <https://hdl.handle.net/1887/19781>

Version: Corrected Publisher's Version

License: [Licence agreement concerning inclusion of doctoral thesis in the Institutional Repository of the University of Leiden](#)

Downloaded from: <https://hdl.handle.net/1887/19781>

Note: To cite this publication please use the final published version (if applicable).

Cover Page



Universiteit Leiden



The handle <http://hdl.handle.net/1887/19781> holds various files of this Leiden University dissertation.

Author: Farenc, Carine

Title: Discovery of small molecules inhibitors of EphA4

Date: 2012-09-13

Chapter 6

Biophysical characterization of fragments discovered with TINS

Major drug discovery efforts for novel targeted therapies of various human malignancies focus on the human kinome. Indeed, modulation of phosphorylation signaling pathways by small molecules has demonstrated considerable clinical efficacy in the treatment of devastating disorders such as cancer. Here we present the biophysical characterization of fragments interacting with the EphA4 receptor. Fragments discovered previously with the Target Immobilized NMR Screening approach, were characterized using Surface Plasmon Resonance (SPR) and [^{15}N , ^1H]-HSQC experiments. We successfully developed a functional SPR assay for EphA4, binding affinities could be determined for several fragments and competition experiments with ATP were undertaken. Our results establish the utility of biophysical methods in the characterization of fragment screening hits.

Introduction

From the approval of the first kinase inhibitor, imatinib⁴⁵, for the treatment of chronic myelogenous leukemia (CML) in 2001 to the approval of vandetanib⁴⁶ in early 2011, protein kinases have developed into one of the most important target classes in oncology drug discovery. However, studies revealed that most approved kinase inhibitors have limited selectivity and target multiple kinases.⁴⁷ EphA4, a receptor tyrosine kinase normally only expressed in the developing brain, was recently found to be highly overexpressed in tumor cells of cutaneous T-cell lymphomas (CTCL),¹⁸⁰ prostate cancer and pancreatic cancer^{58, 181, 182} suggesting that it might be a promising target for pharmacologic intervention. Furthermore, it has been suggested that EphA4 inhibition might be beneficial for the treatment of spinal cord injuries.^{60, 202}

Over the last decade, fragment based drug Discovery (FBDD) has been recognized as a powerful strategy to develop novel, small molecule drugs.^{105, 203} FBDD screens small libraries (1,000 - 20,000 compounds) of so-called drug “fragments” that are typically described by a “rule of threes”²⁸ (Ro3, Mr < 300 Da, cLogP < 3, H-bond donors < 3, H-bond acceptors < 3, number of rotatable bonds < 3 and TPSA (total polar surface area) < 60 Å²) for binding to the target. The crucial step in this drug discovery process is the reliable identification of the initial fragments that typically interact only weakly with the receptor due to their small size. Several biophysical methods such as NMR,^{126,27} protein crystallography²⁰⁴ and surface plasmon resonance (SPR)²⁰⁵ have been employed to identify such weak protein ligand interaction.

We have developed an NMR ligand screening approach, called Target Immobilized NMR screening (TINS) and have used the method to screen a fragment library for binding to the kinase domain of the EphA4 receptor (Chapter 3). We wished to compare the results of TINS and biochemical methods to those from alternative biophysical techniques such as Surface Plasmon Resonance (SPR) and [^{15}N , ^1H]-HSQC (Heteronuclear Single Quantum Correlation) experiments. Thus the binding of all fragments discovered in Chapter 3 was studied by SPR. In addition, protein observed NMR was used to study the binding of fragments to the EphA4 KD under conditions similar to those used for crystal soaking (Chapter 3 and 5).

Materials and method

Protein purification for Surface Plasmon Resonance studies

The enzymatically biotinylated AVI-KD of EphA4 was purified as described in Chapter 3, while the 6His fusion KD of EphA4 was purified as described in Chapter 4.

Immobilization for Surface Plasmon Resonance studies

All SPR studies have been performed using a Biacore T-200 instrument (GE Healthcare). Sensor Chip CM5 and NTA and the amine coupling kit were purchased from GE healthcare. All buffers were freshly prepared and filtered through 22 μm membranes.

Immobilization of the 6His-Kinase Domain of EphA4:

Capture was performed at 15 °C by injecting the His kinase fusion protein over a Ni-NTA chip previously charged with 0.5 mM NiCl₂ at 10 $\mu\text{l}/\text{min}$ for 5 min. The chip was regenerated with 1 M imidazole, followed by 350 mM EDTA and 2 M NaCl at 20 $\mu\text{l}/\text{min}$. Injections were repeated until saturation or until the desired level was reached. The running buffer used in all subsequent binding and inhibition experiments was composed of 20 mM Tris Buffer, 200 mM NaCl, 1mM MgCl₂, 0.05% Tween 20, pH 7.5 with 5% of DMSO. On average, 3000 response units (RUs) of 6His-EphA4 were immobilized.

Immobilization of the biotinylated Kinase Domain of EphA4:

Coupling of NeutrAvidin (PierceNet Thermo Scientific) to the CM5 surface was performed using the amine coupling kit from GE healthcare according to the instructions of the manufacturer. In brief, NeutrAvidin was first dissolved (10 mM HEPES pH 7.5, 50 mM NaCl and 0.01% Tween 20) at a concentration of 50 μ M and then diluted to 5 μ M in 10 mM Na-acetate buffer at pH 4.8. The functional groups of the CM5 chip surface were first activated by injecting a mixture of carbodiimide (0.5 M) and N-hydroxysuccinimide (0.5 M), immediately followed by injecting the NeutrAvidin at a flow rate of 5 μ l/min. The remaining activated carboxyl groups on the surface were blocked with 50 μ M sodium hydroxide. Approximately 7500 response units (RUs) of NeutrAvidin were immobilized. The running buffer used in all subsequent binding and inhibition experiments was composed of 20 mM Tris Buffer, 150 mM NaCl, 2 mM MgCl₂, 0.05% Tween 20, pH 7.5 with 5% of DMSO. The biotinylated protein was immobilized at a concentration of 5 μ M for 5 min at 10 μ l/min resulting in approximately 13000 RU of protein immobilized. As a reference, biotin was immobilized in the same conditions, reaching an immobilization level of approximately 80 RU.

Analysis of fragment-EphA4 KD interactions by SPR biosensor

Equilibrium binding experiments:

A 100 mM stock solution of each compound in 100% DMSO was diluted into the running buffer to obtain an aqueous fragment solution at 750 μ M concentration

containing 5% DMSO. For compound **27** from chapter 5, the stock solution of 500 μM in 100% DMSO was diluted to 25 μM . For titration experiments, samples were injected in a series of 6 concentrations with a maximum of 750 μM or 1500 μM with the exception of compound **27** for which titrations were run with a maximum of 50 μM . These solutions were injected over the protein sensor surface for 25s at a flow rate of 30 $\mu\text{l}/\text{min}$ and after every 25 injections the reference compound **27** was injected as a control at a single concentration of 25 μM . In addition, titrations of compound **27** were performed at the beginning and at the end of each plate, in order to assess the stability of the surface. These control measurements were performed to check both the stability and ligand-binding activity of the immobilized proteins during a screen. SPR experiments using the 6His fusion KD were performed at 15°C and those using the biotinylated KD were performed at 20 °C. For the 6His fusion KD screen, regeneration of the surface between subsequent binding experiments was achieved by washing the surface extensively (30 s) with the running buffer plus 10% DMSO. Sensor responses were taken during each injection after a contact interval of 30 s. Report points at 5 seconds before the end of the injection were used for analysis.

Data analysis:

All sensorgrams were processed using a double-referencing method.²⁰⁶ First, the binding response from the reference surface was subtracted from the binding response from the surface containing EphA4 to correct for bulk refractive index changes. Second, the response from an average of the blank injections was subtracted to remove any systematic artifacts observed between the reaction and reference flow cells.

Assuming linearity between molecular weight and refractive index, the percentage of active protein immobilized could be estimated from the saturation response of the reference compound (**27**) according to equation 1.

$$R_{\max} = \frac{MW_{\text{comp}}}{MW_{\text{prot}}} \times R_{\text{prot}} \quad (1)$$

R_{\max} is the saturation signal determined for the reference, R_{prot} is the signal measured for the amount of immobilized protein [RU], and MW_{comp} and MW_{prot} are the respective molecular weights of reference compound and protein.

Data was fitted using GraphPad Prism version 5.00 for Windows, GraphPad Software, La Jolla California USA. The K_D value could be estimated using equation (2) derived from the Langmuir adsorption isotherm.

$$K_D = \frac{R_{\max} \times C}{R} - C \quad (2)$$

R_{\max} , R , and C correspond to the normalized saturation response of the reference compound, the normalized response of the test compound, and the concentration of the test solution, respectively.

Competition experiments:

The competition experiments were performed by sequentially injecting the solution of the test compound (fragment), the reference compound at saturation concentration i.e. ATP (500 μM), and a mixture of fragment and reference compound each for 30 seconds. The test compounds were compound **27** (2 μM), compound **44** and **7**

(750 μM). A qualitative comparison of the signals observed for test compound, reference compound and mixture was then performed. For competition, experiments the running buffer was 20 mM Tris Buffer, 150 mM NaCl, 10 mM MgCl_2 , 0.05% Tween 20, pH 7.5 with 5% of DMSO. In addition, a titration of ATP was performed. Samples were injected in a series of concentrations with a maximum of 1000 μM .

The evaluation of competitiveness in this experiment required specific data analysis. Fragments displaying high affinity relative to the competitor and binding to the same binding pocket as ATP, showed a signal for the mixture (ATP + fragment) that was identical to the signal observed for the fragment alone. In the case of low affinity fragments, where saturation was difficult to reach, the response that would be observed if the compound is competitive with ATP for binding to EphA4 (i.e. binds to the ATP binding pocket) is given by the sum of the fractional occupancies (FO) of ATP and the fragment. The fractional occupancies of the mixture of the 2 compounds can be calculated using equations 4 and 5.²⁰⁷

$$FO(A) = \frac{1}{1 + \frac{K_D(A)}{C_A} \left(1 + \frac{C_B}{K_D(B)} \right)} \quad FO(B) = \frac{1}{1 + \frac{K_D(B)}{C_B} \left(1 + \frac{C_A}{K_D(A)} \right)} \quad (4)$$

$K_D(A)$ and $K_D(B)$ are the equilibrium dissociation constants of the competing compounds, and C_A and C_B are the respective concentrations. In the case of competition between compounds of similar affinity and equal concentration, the occupancy of the binding sites by one of the components is heavily influenced by the presence of the other. From the estimation of the occupancies, the expected signals of the 2 compounds could be estimated using equation 5.

$$R_{observed} = FO(A) \times R_{max}(A) + FO(B) \times R_{max}(B) \quad (5)$$

in which $R_{\max}(A)$ and $R_{\max}(B)$ are the saturation responses of the 2 compounds and $FO(A)$ and $FO(B)$ are the respective fractional occupancies.

Protein production for NMR studies

The plasmid pET28b containing the kinase domain of EphA4 (amino acids 606-846) was transformed in *E. coli* BL21 RP competent cells. The cells were incubated overnight at 37°C on a LB/Kan/Cam (0.05 g/l Kanamycin, 0.034 g/l Chloramphenicol) plate. A single colony was inoculated in 50 ml M9 minimal medium supplemented with 0.3 g/l $^{15}\text{NH}_4\text{Cl}$ and 0.05 g/l Kanamycin, 0.034 g/l Chloramphenicol in a 250 ml flask. Five mL of the pre-culture was inoculated in 0.5 L M9 minimal medium (0.3 g/l, $^{15}\text{NH}_4\text{Cl}$, 0.05 g/l Kanamycin, 0.034 g/l Chloramphenicol). The cultures were grown at 37°C, shaking at 250 rpm to an OD_{600} of 0.6 before induction with 0.1 mM IPTG. At the same time the temperature was lowered to 18°C and growth was continued overnight before harvesting. A cell pellet corresponding to 1 liter of culture was resuspended in 30 ml of lysis buffer (50 mM Sodium phosphate pH 8.0, 300 mM NaCl, 20 mM imidazole, 0.05% Tween 20, 10% glycerol and 0.01% beta-mercapto-ethanol) supplemented with a protease inhibitor cocktail (complete EDTA-free) from Roche, lysed using a French press and centrifuged at 37,000 x g for 45 min at 4°C. The supernatant was applied to a 5 ml HisTrap HP column (GE Healthcare) with a peristaltic pump at 4°C for 1 hour (Binding buffer: 20 mM Tris-HCl pH 7.6, 500 mM NaCl and 5 mM imidazole). After extensive washing, the recombinant protein was eluted with binding buffer plus 500 mM imidazole.

The 6His fusion EphA4 was incubated with 20 mM ATP and 20 mM MgCl₂ in order to fully activate it. After an hour at 4°C, the protein was diluted 10 fold in 10 mM HEPES pH 7.5, 10 mM NaCl and applied to a 1 ml HiTrap Q column (GE healthcare) that had been pre-equilibrated with the same buffer. The fractions containing the EphA4 kinase domain, which did not bind to the column, were then concentrated to 5 ml and applied to a Sephacryl S-200 HR column (HiPrep 16/60; GE Healthcare) equilibrated in 10 mM HEPES, 500 mM KCl and 1 mM DTT.

NMR sample preparation

The 6-His fusion KD was concentrated using a Centricon-10 (Amicon). All protein samples contained identical buffer condition 20 mM HEPES, 150 mM NaCl, 2 mM DTT, pH 7.2, in 3% D₂O. The sample for recording the apo protein spectra contained 80 μM ¹⁵N-6His-KD. The sample for pH titration contained 100 μM of protein and the pH, ranging from 5.8 to 6.2, was adjusted with 0.1 M HCl or 0.5M NaOH. The samples for compound titration contained 100 μM of protein in buffer and 100 mM stock solutions of compounds **27**, **3** and **5** were prepared in *d*₆-DMSO.

NMR Spectroscopy

All NMR spectra were recorded at 298 K on a Bruker DMX600 spectrometer. [¹⁵N,¹H]-HSQC were obtained with spectral widths of 28 ppm (¹⁵N) and 16.0 ppm (¹H). Data was processed with Topspin 2.1 and analyzed with Sparky.²⁰⁸

Results

Development of SPR biosensor assay for EphA4

Initially, the same immobilization strategy as the one used for TINS studies (*c.f.* Chapter 3), *i.e.* immobilization *via* the SNAP affinity tag was used for SPR biosensors studies. As a reference, the SNAP protein was immobilized in a separate channel. To establish the validity of the SPR assay, a well-characterized ligand was first titrated. As compound **27** was biochemically validated and the 3D structure was available (*c.f.* Chapter 5), this compound was chosen as a reference. However, the titration of compound **27** did not exhibit a concentration dependent response (Data not shown) suggesting that the SNAP mediated immobilization strategy was not suitable for SPR studies.

As an alternative,, we attempted to immobilize the KD of EphA4 via the oligo histidine tag on an Ni-NTA sensor chip. Purified 6His fusion KD was captured on the sensor chip and a titration of compound **27** was performed (Fig. 6.1). As seen in Fig. 6.1A, binding of **27** to the metal affinity immobilized KD was dose responsive and saturated at an appropriate level. The binding affinity of compound **27** was determined using equation (2) derived from the Langmuir adsorption isotherm (Fig. 6.1A). Analysis of the titration data indicates that compound **27** binds with an affinity of 1 μM which is comparable with the affinity measured by biochemical assay ($\text{IC}_{50} = 4.5 \mu\text{M}$, *c.f.* Chapter 5). The IC_{50} of compound **27** is slightly higher than the K_D , this was expected given that the inhibitor competes with ATP for the same binding site in the activity assay.

The kinetic association (k_a) and dissociation (k_d) constants for binding of **27** to immobilized EphA4 could be determined by fitting the data to a 1:1 binding model. The fitting yielding values of $k_a = 2 \times 10^5 \text{ M}^{-1}\text{s}^{-1}$ and $k_d = 0.5 \text{ s}^{-1}$ (Fig. 6.1B). The resulting kinetically determined dissociation constant K_D , of 2 μM matches the equilibrium affinity determined from the Langmuir isotherm.

The binding curve in Figure 6.1 indicates that the saturation response for compound **27** is approximately 18 RU. Using the molecular weight of the immobilized protein and reference compound **27** (37,282 Da and 296 Da respectively) and the amount of immobilized protein (R_{prot}), the theoretical saturation response for 100% active protein is estimated to be 29 RU according to equation (1). Comparing the theoretical and experimental saturation responses, the percentage of immobilized protein that was active for ligand binding was estimated to be about 63%. Other known ligands such as ATP and ADP were assayed, but no binding was observed and therefore compound **27** was used as a reference for monitoring the stability of EphA4 during the SPR assay.

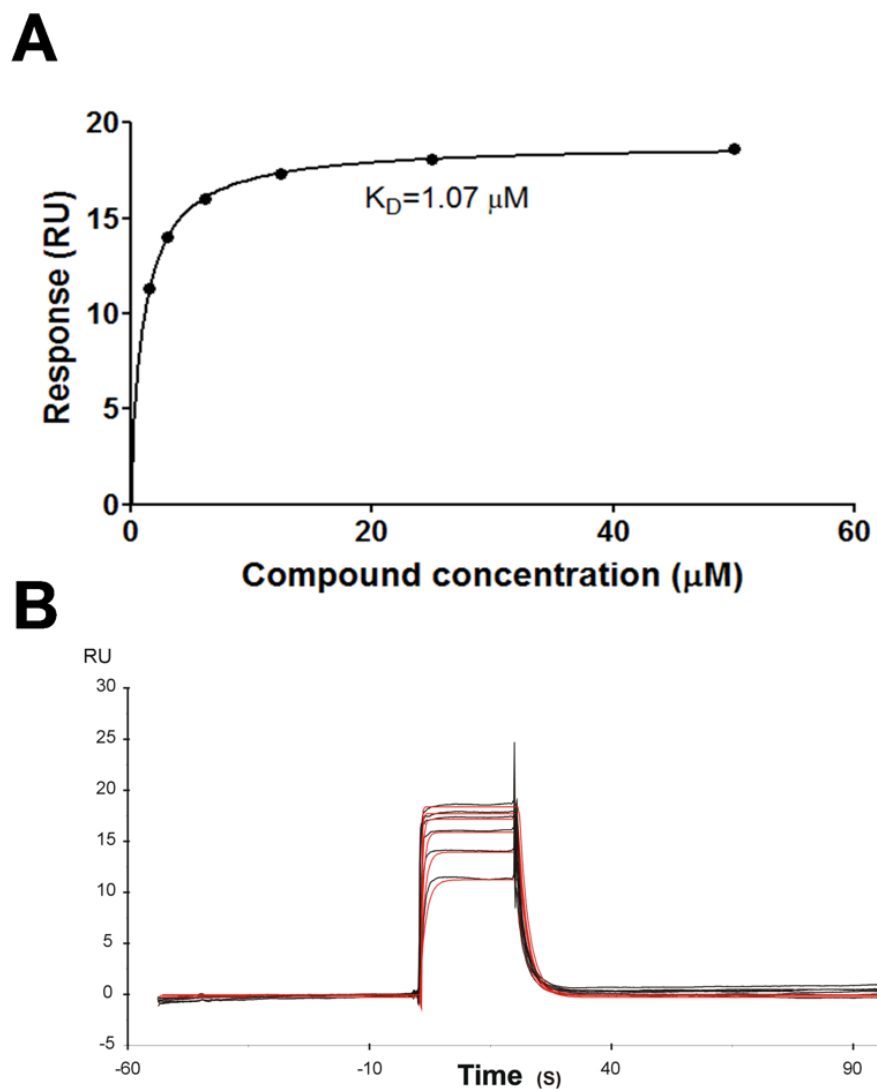


Figure 6.1: SPR characterization of compound **27** binding to EphA4 6His-KD. A) Representative saturation curve of compound **27** binding. The response signal is plotted against the concentration of compound **27**. B) Sensorgrams measured at the following concentrations: 1.56, 3.125, 6.25, 12.5, 25 and 50 μM . The sensorgrams were processed using the double referencing method. The red lines overlaid on the experimental black curves result from the fit of the experimental data with the Biacore T200 evaluation software (version 1.0) using the mathematical function of a kinetic 1:1 binding model.

Biophysical characterization by SPR of hits from SNAP fusion KD TINS screen

Initially, compounds from the TINS screen of the SNAP fusion KD were selected and biochemically characterized (*c.f.* Chapter 3). We wished to compare the biochemical results to the SPR results. The SPR experiment was carried out on the 6His KD of EphA4 immobilized on an NTA chip and 134 compounds were assayed at a single concentration of 750 μM . In order to compare the results from the SPR assay to the biochemical assay and the ligand screening results from TINS, compounds were categorized in groups for more clarity (Table 6.1). Compounds considered as hits in the TINS screen (for more details refer to Chapter 3) and demonstrating biological activity were classified in group I. Group II contained hits from the TINS experiment but that did not show biological activity. Fragments that exhibited inhibition in the enzymatic assay but were not considered as hits in TINS screen belonged to group III. Finally, negative controls i.e. compounds that did not show either binding in TINS experiment nor biological activity, were classified in group IV.

Table 6.1: Comparison of hits from TINS, biochemical assay and SPR. In the TINS screen of SNAP KD fusion, compounds were selected as binders when the T/R was lower than 0.4 (Chapter 3, fig. 3.5). For the enzyme inhibition assay, compounds were considered as inhibitors when the PIN was above 10 % (Chapter 3, table 3.1). Regarding the SPR experiments, fragments were identified as hits when the signal exceeded 3 times the SD and lower than the maximal theoretical response (see below).

	Group I	Group II	Group III	Group IV
	+ TINS +E.I	+ TINS -E.I	-TINS +E.I	- TINS -E.I
SPR positives	6	63	1	3
SPR negative	6	48	1	6
Total of compounds	12	111	2	9

E.I.: Enzyme inhibition assay

Fragments were identified as hits in the SPR assay when the signal exceeded 3 times the noise and the response was lower than the maximum theoretical response at saturation (i.e. binding was 1:1). Ill-behaved compounds were eliminated if they showed evidence of super stoichiometric binding, precipitation and/or a sensorgram that indicates non-equilibrium behavior.²⁰⁹ Using these criteria, 73 out 134 compounds were considered as hits in this SPR assay.

Half of the compounds from group I and a majority of compounds from group II were categorized as binders in the SPR assay suggesting a correlation between the SPR experiment and the TINS assay. As the detection window was quite small (11 RU in the present experiment), some compounds may not have been positive in the SPR assay due

to insufficient sensitivity. Moreover, the extremely high sensitivity of TINS (up to ~ 20 mM K_D)¹⁴⁹ allows identification of many compounds that may not be detected in the SPR assay which has an upper limit of 2-5 mM under ideal conditions.²¹⁰

Of the compounds from group II that were hits in TINS and biochemically negative, 63 were confirmed as hits in the SPR experiment suggesting that either these compounds bind too weakly to inhibit or that they bind at a non-biologically productive site. Out of the two compounds from group III, one fragment that was negative in TINS but positive in the bioassay was detected as positive in the SPR experiment. This compound was deemed to be a false negative for TINS. Interestingly, the other compound which was negative in both TINS and SPR, showed activity in the biochemical assay, possibly suggesting that the compound was a false positive in the biochemical assay. The 3 compounds in group IV categorized as positive in the SPR experiments are probably false positives.

In order to gather more biophysical information, the 73 well behaved compounds from the single concentration SPR assay were subsequently titrated. Compounds exhibiting low response at 750 μ M (i.e. less than $0.5 \times$ the R_{max} observed for compound **27**) were titrated using a concentration range from 46 μ M to 1500 μ M. Meanwhile, compounds exhibiting a higher response in the single concentration assay were titrated using a concentration range from 23 to 750 μ M. Out of these 73 compounds, 12 presented a clear concentration-dependent response. The binding affinity of these fragments was estimated by SPR to range from 0.75 to 3 mM (Appendix C). Out of these 12 fragments, 3 were from group I and 9 from group II. Compounds from group III and IV were titrated but did not show any concentration dependent response.

For compounds **2**, **3** and **8** from group I *i.e.* positive in the TINS screen and biochemical assay, the binding affinities were estimated to be 800 ± 400 , 900 ± 400 , 1100 ± 700 μM (Fig. 6.2). The measured responses were analyzed using a non-linear method derived from the Langmuir model and points where the binding was less than 5% of the maximum response are considered to be highly inaccurate and were ignored.²¹¹ The large uncertainty derives from the fact that binding could not be saturated.

It is known that the NTA surface has the inherent problem of leaching of the immobilized protein which leads to a “drooping” baseline.²¹² Consequently, it was difficult to determine with precision the binding affinities for many of the compounds analyzed. Despite a highly variable level of immobilization (between 1500 and 3000 RU, also frequently encountered with this immobilization strategy) and the leaching off the surface, useful data was still achieved and a rough estimate of the binding affinity could be determined for a few compounds. Nonetheless, a more stable system with a larger response window would clearly be advantageous.

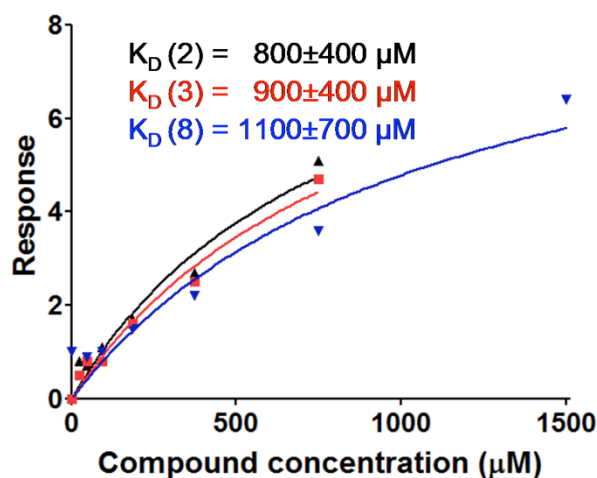


Figure 6.2: SPR analysis of fragment binding to EphA4 KD immobilized via the 6His tag. Representative saturation curves of compounds **2**, **3** and **8** from Group I compounds. The response signal is plotted against the concentration of compound.

Biophysical characterization by SPR of hits from the Biotinylated KD TINS screen

To further characterize the hits selected during the TINS ligand screen of the biotinylated KD, binding to EphA4 was characterized by SPR using the same immobilization approach as used in TINS. The kinase domain of EphA4 was enzymatically biotinylated at the AVI tag and captured on a biosensor chip *via* immobilized NeutrAvidin. To validate the assay, the binding of compound **27** was monitored and results were compared to those from the immobilization using the 6His tag (Data not shown). The K_D of **27** for biotin immobilized EphA4 KD was estimated to be $\sim 1.9 \mu\text{M}$ and the percentage of active protein was approximately 95%. This binding affinity for compound **27** is similar to the one obtained with the 6His KD immobilization on the NTA chip ($1.9 \mu\text{M}$ for the present immobilization compared to $1\text{-}2 \mu\text{M}$ for the immobilization on NTA chip) while the percentage of active protein is significantly higher. Further comparison of the two immobilization methods is presented below.

A total of 62 compounds was selected as hits in the TINS experiment using biotinylated EphA4 (c.f. Chapter 3) and assayed for binding at a concentration of $750 \mu\text{M}$ *via* SPR technology. Of these 62 compounds, 51 were positive for binding in the SPR experiment, while 11 did not show binding, giving an 82% validation of the selected TINS hits. The well-behaved compounds (as previously defined) amongst the 51 binders were further analyzed to determine their equilibrium binding affinity by titration experiments. Reproducible, concentration dependent curves were obtained for 8 compounds. Examples of the experimental binding curves are shown in Figure 6.4 for compounds **7** and **44** and in Appendix D for the remaining compounds. Binding

affinities of these 8 fragments were estimated to range from 0.4 to 2.6 mM. The binding affinity for compounds **7** and **44** was estimated to be $650 \pm 65 \mu\text{M}$ and $460 \pm 60 \mu\text{M}$ respectively.

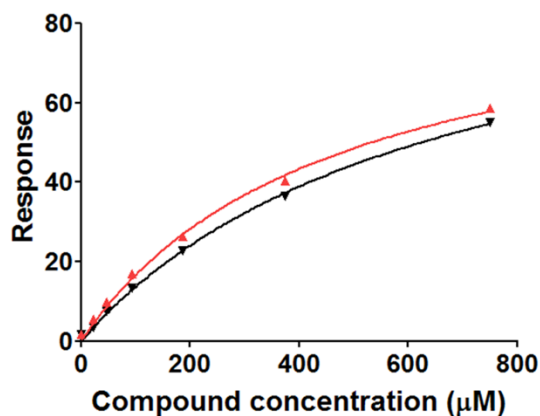


Figure 6.3 SPR analysis of fragments binding to EphA4 KD immobilized *via* NeutrAvidin. Saturation binding curves of compounds **7** and **44**. The response signal is plotted against the concentration of each compound. Compounds **7** and **44** are represented in black and red respectively.

Comparison of the two SPR immobilization approaches

We wished to compare the relevance of the two SPR approaches: immobilization of 6His fusion KD on the NTA chip and ligand capture of biotinylated EphA4. A total of 13 compounds were tested in both SPR assays, 8 were positive in both assays and 3 were negative in both assays. Meanwhile 2 compounds were detected as binding in the SPR assay on the biotinylated KD but not in the 6His SPR assay. One possible explanation resides in the window for ligand detection. In the immobilization mediated with NTA

chip, the level of immobilization was significantly lower than the one in the ligand capture of biotinylated KD (3,000 RU vs. 13,000 RU). This resulted in a smaller window for ligand detection: ~11 RU for 6His KD immobilization vs. ~100 RU for biotinylated KD immobilization. It is likely that the SPR signal for these 2 compounds was close to the noise in the 6His KD immobilization, thus they appeared as false negatives. In addition, compound **32** was titrated using the 2 different immobilization procedures and the binding affinities obtained were very similar. ($K_D \sim 900 \pm 400 \mu\text{M}$ in the SPR screen of the 6His fusion KD and $K_D \sim 900 \pm 600 \mu\text{M}$ in the SPR screen of biotinylated KD).

Competition experiments

Competition binding experiments allow one to differentiate artifactual ligand binding from real binding and can provide insight into the binding site on the target. Given the inability to obtain crystal structures of screening hits bound to EphA4, the information from competition binding experiments could be used to enhance the reliability of computational docking experiments.

Among the compounds titrated using SPR technology, compounds **7** and **44** presented the highest affinity relative to the other fragments. Therefore, these two compounds were assayed for competitive binding with the natural ligand ATP using SPR. Since immobilization via enzymatic biotinylation proved superior, this approach was used to conduct the competition experiments. It was necessary to first demonstrate well-behaved binding of ATP to the immobilized KD. Since kinases typically bind ATP as a complex with Mg^{2+} , MgCl_2 was included in the running buffer and binding of ATP was

now clearly observed. This result suggests that the reason for the lack of ATP binding to the SNAP-KD may have been the absence of Mg^{2+} . ATP was subsequently titrated in order to determine the binding affinity (Fig. 6.4). Binding of ATP to immobilized EphA4 KD was characterized by k_{on} and k_{off} rates that were faster than the maximal detectable rates of the Biacore instrument, as has been previously observed for other kinases²¹³ (Fig. 6.5A). Hence, the K_D value was calculated from the equilibrium response of the ATP injections at various concentrations. The fit of the Langmuir isotherm for ATP (Fig. 6.4B) gave a K_D value of $270 \pm 15 \mu M$.

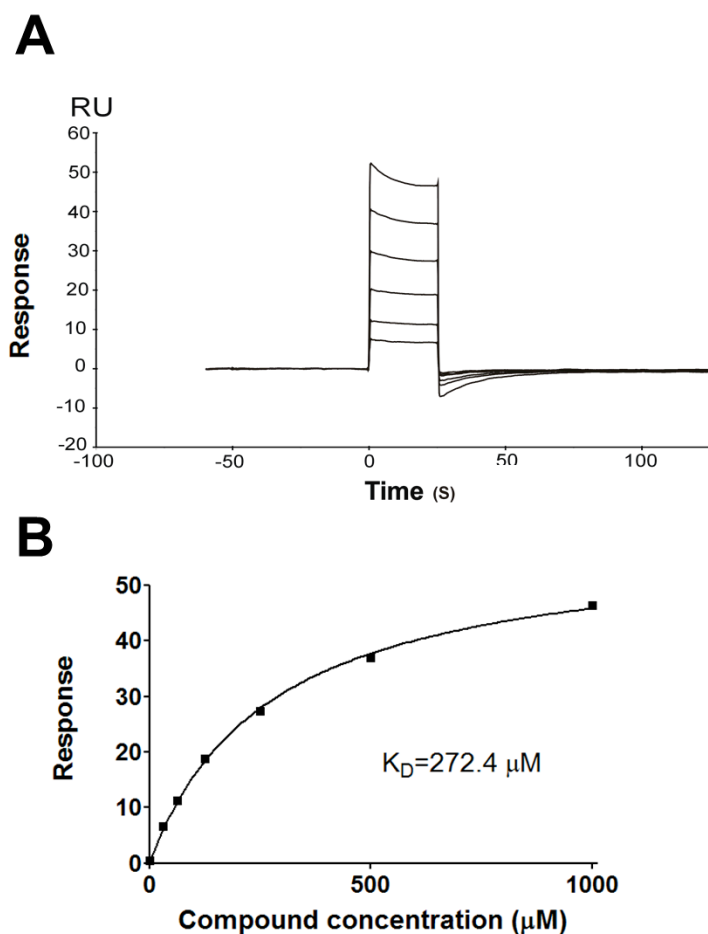


Figure 6.4: A) Sensorgram of ATP binding to immobilized EphA4 KD measured at the following concentrations: 35.25, 62.5, 125, 250, 500 and 1000 μM . B) Representative saturation curve of ATP binding.

Two compounds that simultaneously bind to the KD would be expected to generate an additive binding response in SPR.²¹⁴ In contrast, a compound that binds to the ATP binding pocket would compete with ATP and therefore give a non-additive response in SPR. Based on the crystal structure of compound **27** in complex with EphA4, which showed the compound bound in the ATP binding pocket, this particular compound was chosen to validate the SPR competition binding assay (Fig. 6.5). Compound **27** was tested in the presence and absence of ATP at a saturating concentration. The SPR response observed in the presence and absence of ATP is the same for **27**. This result is what is expected when a 10 fold more potent ligand competes with a weaker ligand, i.e. complete displacement of the weaker ligand.

Figure 6.5 summarizes the results of the competition experiments that were performed with fragments **7** and **44** versus ATP. In these cases, we observe that the signal of the mixture (black bars) is different from the individual signals of compounds **7** and **44** (white bars) or ATP (dark gray bars). It has been shown that in the case of competition between compounds of similar affinity, the occupancy of the binding site lies between the individual occupancies and the sum of the 2 individual occupancies.²⁰⁷ The expected signal of the two compounds could be estimated using equations 4 and 5 in the material and method section.

The response for the mixture (ATP + fragment) was calculated in the case of fragment competing with ATP for the same binding site (R_{calc} competition, light gray bars). To be consistent, the response in case of noncompetition (i.e., in the case of independent binding sites for each of the compounds) was also calculated (R_{calc}

noncompetitive, striped bars). When there is no competition, the expected signal is the sum of the two individual responses observed for the fragments.

For compounds **7** and **44**, the experimental responses for the mixtures ATP + fragment are closer to R_{calc} competition than to R_{calc} non competition (Fig. 6.5) Since the experimental binding response is closer to the expected result for competitive binding within experimental error, the data is strongly in favor of competition and suggest that the binding site of compounds **7** and **44** overlaps with ATP. These results imply that compounds **7** and **44** both bind at the ATP binding site.

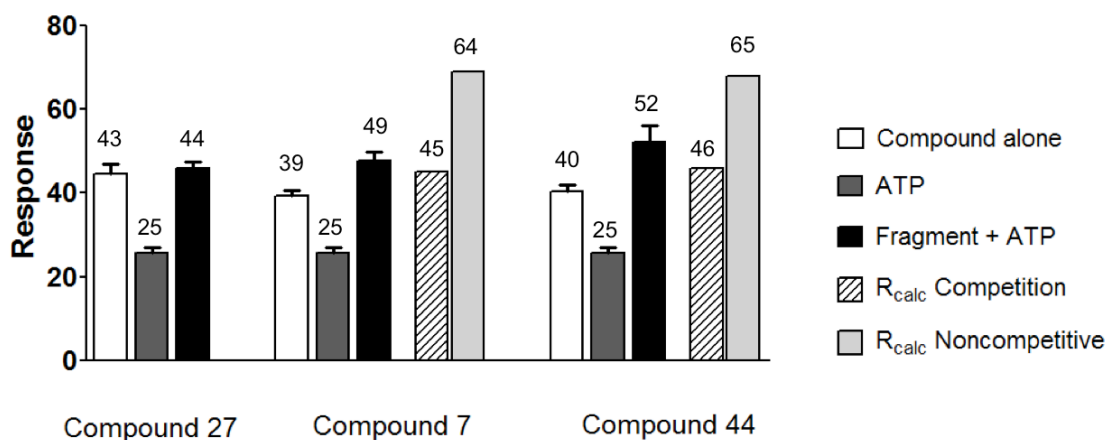


Figure 6.5: SPR analysis of competition binding experiments. The measured response for each compound is indicated by the white bars: compound **27** ($2 \mu\text{M}$) compounds **7** and **44** ($750 \mu\text{M}$), the response for ATP ($500 \mu\text{M}$) by dark gray bars and the response for the mixture (ATP ($500 \mu\text{M}$) + compound ($2 \mu\text{M}$ for compound **27** or $750 \mu\text{M}$ for compounds **7** and **44**)) is shown by black bars. The calculated signal for the mixture (ATP+**7**, ATP+**44**) expected for fractional occupancy of the same binding pocket using the measured affinities and known concentrations, is shown by the striped bars. The calculated signal for the mixture (ATP+**7**, ATP+**44**) expected for different binding pockets (i.e. non-competitive binding) is shown in light gray bars. The mean value is indicated above its respective bar.

NMR characterization of apo-EphA4

Specific binding of a small molecule to a protein will result in concentration dependent, observable changes of the NMR resonances of the protein.²⁷ The most convenient manner to observe these spectral changes is to monitor the amide chemical shifts of a ¹⁵N labeled protein. Chemical shifts of both ¹H and ¹⁵N amide atoms are recorded in the [¹⁵N,¹H]-HSQC (Heteronuclear Single Quantum Correlation) spectrum. In addition, when the sequential assignment of a protein is available, analysis of chemical shifts perturbation data affords rapid access to low resolution structural data to characterize the ligand binding site.^{27, 215} [¹⁵N,¹H]-HSQC NMR titration experiments were used to characterize binding of fragments to EphA4 at a pH equivalent to the one in crystallographic soaking experiments. While the resonance assignment of the kinase domain of EphA4 is not available, spectra of the kinase domain of EphB2 are of high quality, resulting in a complete backbone resonance assignment for this protein.¹³³ The [¹⁵N,¹H]-HSQC spectrum of uniformly ¹⁵N labeled EphA4 protein in the apo-form is presented in Fig. 6.7. The spectrum displayed good resonance dispersion, however the spectrum was sufficiently different from that of EphB2 that the assignments could not be readily transferred. Even in the absence of assignments, chemical shift perturbation studies can be used to characterize binding of a fragment to a protein.

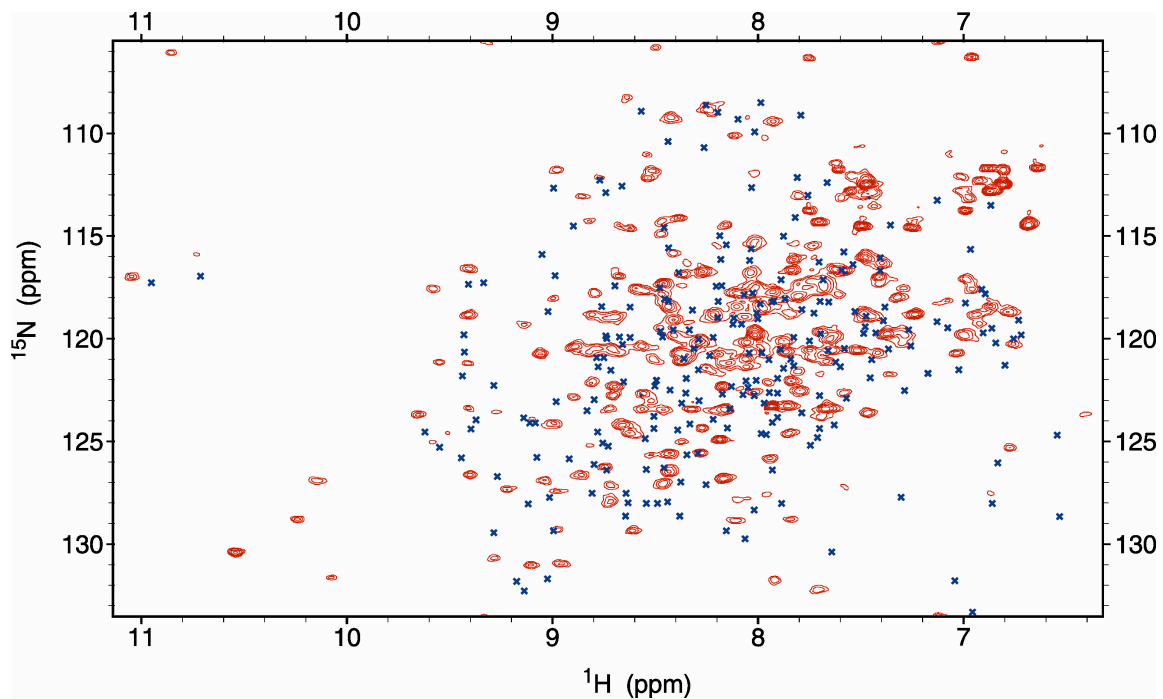


Figure 6.7: $^{15}\text{N}, ^1\text{H}$ -HSQC spectrum of 80 μM ^{15}N EphA4-KD. The resonance frequencies of the $^{15}\text{N}, ^1\text{H}$ -HSQC spectrum of EphB2-KD are represented by blue crosses. No clear correlation between the spectra is observed

pH titration of ^{15}N EphA4 KD

Since it is well known that even small changes in pH can cause changes in the $^{15}\text{N},^1\text{H}$ -HSQC spectrum, it was important to first assess the sensitivity of EphA4 to pH. To do so the pH was titrated in small increments while monitoring the protein by $^{15}\text{N},^1\text{H}$ -HSQC NMR. Spectra were acquired at pH 5.8, 6.0, and 6.2 in order to investigate the possible effect of small changes to the pH used for crystal soaking (pH 6) potentially caused by titration of ligands to high concentration. The superimposition of the $^{15}\text{N},^1\text{H}$ -HSQC spectra at various pH values is presented in Appendix E, while the region showing peaks used for analysis of ligand binding is presented in Figure 6.8. There were no significant chemical shift differences observed in this pH range.

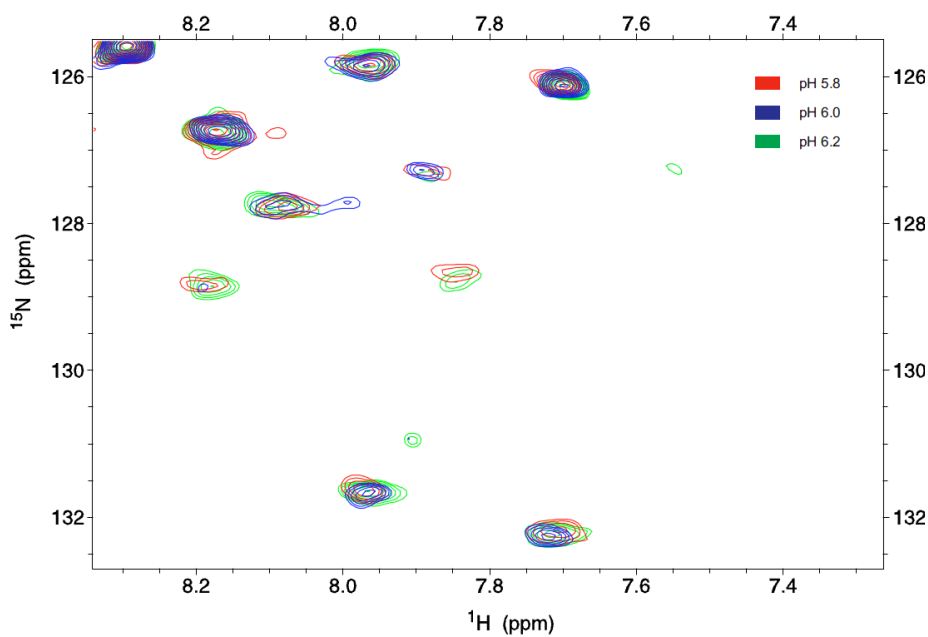


Figure 6.8: pH titration of ^{15}N EphA4 KD. A region of the overlaid $^{15}\text{N},^1\text{H}$ -HSQC spectra of 100 μM EphA4 KD is recorded at pH 5.8, 6.0 and 6.2. This region shows peaks used for analysis of ligand binding.

Titration of compound 27

Initially the well characterized ligand **27** was used to assess the effect of compound binding on the [¹⁵N,¹H]-HSQC spectrum of EphA4. Addition of compound **27** to ¹⁵N EphA4 KD resulted in significant changes in the [¹⁵N,¹H]-HSQC spectrum. The resonances exhibiting the largest changes upon compound **27** binding are shown in Figure 6.9 while the full spectra are presented in Appendix F. We observe that upon addition of compound **27**, peaks 1-3 exhibit significant changes in resonance position that are primarily indicative of slow exchange (that is $k_{\text{off}} \ll \Delta(\delta_{\text{bound}} - \delta_{\text{free}})$). On the other hand, peak 4 showed both a gradual decrease in peak intensity and concentration dependent chemical shift change, suggesting intermediate exchange (that is $k_{\text{off}} \approx \Delta(\delta_{\text{bound}} - \delta_{\text{free}})$). As the resonance assignment of EphA4 is not available, these 4 peaks, which report on ligands binding at the ATP site, are simply referred to by number. Since the binding of **27** to EphA4 could readily be detected, it was deemed worthwhile to investigate the binding of fragment screening hits using this approach.

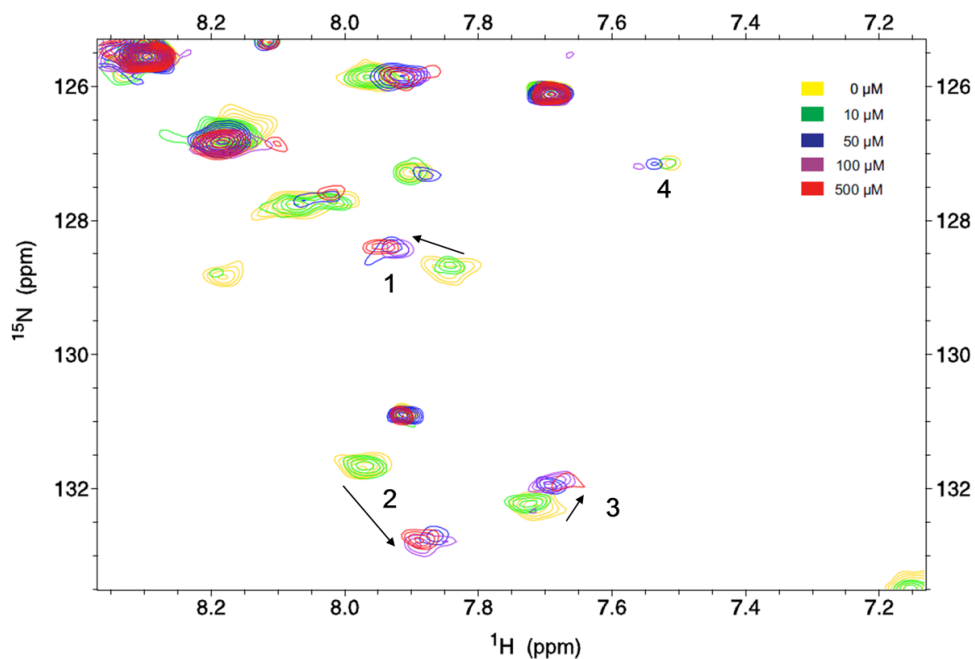


Figure 6.9: NMR analysis of compound **27** binding to ^{15}N EphA4 KD. A region of the overlaid $[\text{}^{15}\text{N},\text{}^1\text{H}]$ -HSQC spectra of 100 μM of ^{15}N EphA4-KD with increasing concentration of compound **27** is shown. Peaks whose resonance position changes with increasing concentration of compound **27** are indicated with arrowheads and numbers.

Fragment binding to ^{15}N EphA4 KD

Perturbations in the spectrum of EphA4 KD were monitored upon addition of different fragments. For clarity, we focused on a small region of the spectrum containing peaks reporting on binding to the ATP pocket as determined from the titration of **27** (Fig. 6.10). We selected compounds **3** and **5** from the TINS screen of the SNAP fusion KD since they were also active in the enzyme inhibition assay yet negative for crystallography. Figure 6.11, shows that upon addition of compound **3**, peaks 2 and 3 are shifted, meanwhile in presence of compound **5** peaks 1 and 3 are shifted. The same peaks are shifted in the presence of compound **27** (Fig 6.11B) and these peaks are not related to

a change in pH (Fig. 6.11C). It is likely that compounds **3** and **5** bind in a similar site as **27** *i.e.* in the ATP binding site.

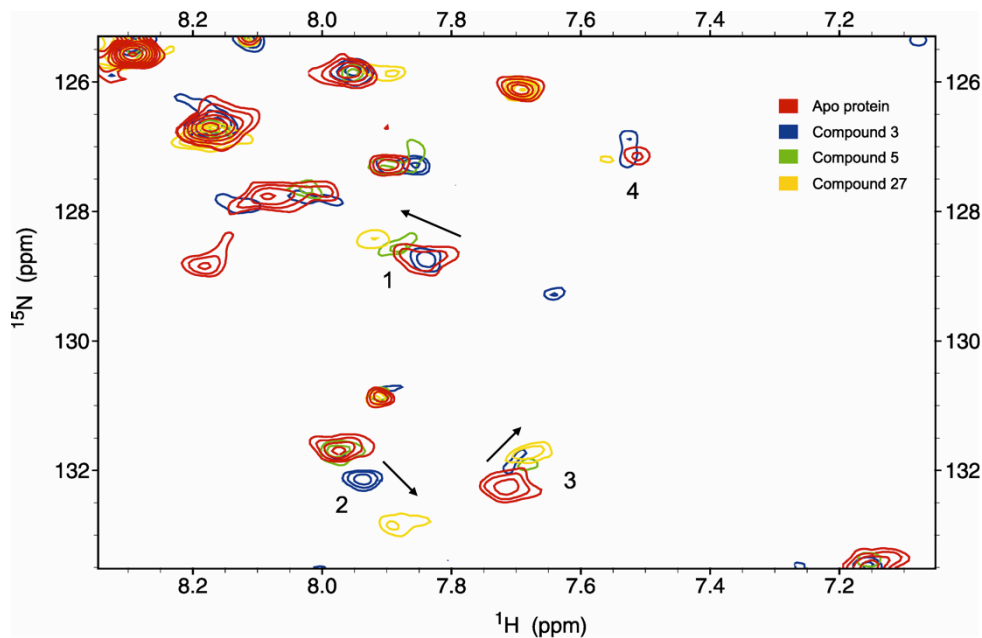


Figure 6.10: NMR analysis of ligand binding to EphA4-KD. A region of the overlaid $^{15}\text{N}, ^1\text{H}$ -HSQC spectra of 100 μM apo ^{15}N EphA4-KD and in the presence of the indicated compounds is presented. Compound **3** (blue) and compound **5** (green) were added to 2 mM and compound **27** (yellow) was added to 100 μM . Peaks whose resonance position changes with increasing ligand concentration are indicated with arrowheads and numbers.

Discussion

The initial plan of this collaborative research project was to develop potent, specific inhibitors of EphA4 kinase activity using both computational and experimental approaches. As we have seen, the computational approach has led to a reasonably potent and specific compound (**27**) for which a crystal structure has been elucidated bound to EphA4. Surprisingly, the experimental approach of using a biophysical assay for ligand screening and confirming with a biochemical assay has failed to yield a single compound for which a crystal structure could be determined. Moreover, several fragment screening hits were selected for elaboration studies but these did not lead to compounds with similar potency as **27**. There are a number of possible explanations for these observations. One is that the form of the protein that was screened using TINS was not biologically relevant. A second is that the biochemical assay was not functioning as a proper filter to differentiate real from artifactual binding. The experiments described in this chapter aimed to determine whether either of these explanations were correct.

Surface Plasmon Resonance (SPR) was employed to provide orthogonal biophysical characterization of the compounds binding to EphA4. To obtain high quality SPR data, the target protein has to be immobilized in a way that maintains its activity. The SPR characterization was conducted with 2 different recombinant proteins (6His fusion KD and biotinylated AVI fusion KD) using 2 different mechanisms of protein immobilization (via Ni-NTA surface and NeutrAvidin immobilized on CM5 surface). As compound **27** was biochemically validated and the binding mode was confirmed by crystallography (*c.f.* Chapter 5), this fragment was chosen as a reference compound for

all SPR studies. The kinetics for compound **27** binding to EphA4-KD immobilized via both methods were fit to a 1:1 binding model yielding kinetic constants $k_a=2 \times 10^5 \text{ M}^{-1}\text{s}^{-1}$ and $k_d=0.5 \text{ s}^{-1}$, and a $K_D \sim 1.5 \pm 0.5 \text{ }\mu\text{M}$. This binding affinity is comparable with the affinity measured by biochemical assay ($\text{IC}_{50}= 4.5 \text{ }\mu\text{M}$, *c.f.* Chapter 5). The data suggested that both immobilization protocols resulted in an SPR assay capable of characterizing small molecules binding to immobilized EphA4 KD. However, immobilization of biotinylated KD presented several advantages when compared to immobilization of the 6His fusion EphA4 KD: (i) the level of immobilization is significantly higher yielding a greater window to study compound binding, (ii) 95% of the calculated binding capacity is retained and (iii) immobilization *via* the biotin NeutrAvidin interaction is more stable.

Compounds selected as hits from the TINS screen were characterized by SPR using both Ni-NTA and biotinylated KD mediated immobilization. Overall, there was a good correlation between the results from TINS screen and the SPR characterization. Approximately 55% of the hits from the TINS screen on the SNAP-KD protein were determined as binders in the SPR assay, while 82% of TINS hit from the screen of the biotinylated KD were validated. Several compounds that were positive for binding in TINS may have been negative in SPR experiments due to the limited sensitivity of the method. It has been shown that dynamic range limitations of SPR can lead to false negatives.¹⁰⁰ In SPR experiments, the observed response is directly proportional to the ratio $[\text{L}]/K_D$. The lower limit of $[\text{L}]/K_D$ leading to a detectable response is in the order of 0.2.²¹⁶ Since concentrations higher than 0.75-1 mM of ligand tend to lead to poor behavior in the Biacore instrument, the practical cutoff for ligand affinity is $\sim 4 \text{ mM}$.

Compounds with weaker affinity than this will appear as false negatives in the SPR experiment.

Subsequently well behaved fragment with reproducible curves that showed clear dose–response and the same qualitative sensorgram shape for each concentration were selected for titration. The binding affinities of several fragments could be estimated and ranged from 0.4 to 3 mM, approximately. However, the binding affinity could not be obtained for a majority of the compounds. There are several possible explanations for this observation. One is that the fragments were too weak and thus saturation could not be reached. In some case compounds may have exhibited promiscuous binding *via* a concentration-dependent aggregation mechanism.²⁰⁹ In addition, it may also have been possible that the stringent curation of the dose–response curves may have resulted in some false negatives.²¹⁰

The fragments with highest affinity and best SPR behavior were assessed for competition binding using ATP. The two compounds, **7** and **44**, were originally selected from the two different TINS screen of EphA4 KD. Compounds **7** and **44** had reasonable ligand efficiencies of 0.3 and 0.25 ($\Delta G/\#$ of heavy atoms) respectively and were likely to bind in the ATP binding site. In principle these compounds could form starting points for hit to lead studies to generate novel EphA4 inhibitors. Interestingly, compound **7** has a very similar structure to compound **27** (Figure 6.11) and the affinity is similar to precursors of **27** that lack the attached derivatized benzene ring. The X-ray crystallographic structure of **27** showed that it binds the hinge region of the ATP binding site. Based on the similarity to compound **27**, it seems likely that compound **7** exhibits a

closely related binding mode to EphA4 KD, that is, it forms hydrogen bonds to the backbone atoms of the hinge residues.

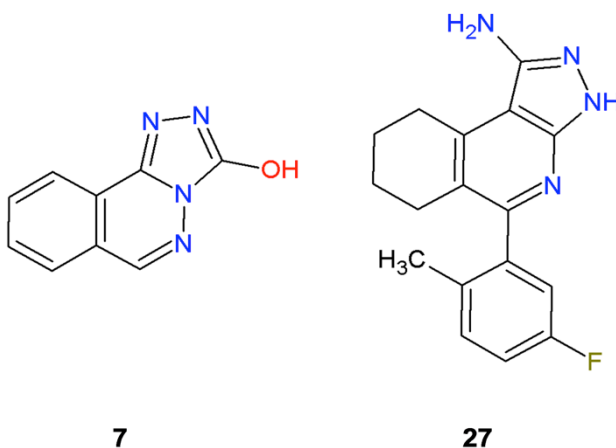


Figure 6.11: Structures of compound **7** (left) and compounds **27** (right).

In order to investigate whether the low yield of fragment structures obtained with X-ray crystallography was related to the difference in pH between screening and biochemical characterization on the one hand and crystallography on the other, protein observed NMR was employed. [¹⁵N,¹H]-HSQC spectra of EphA4-KD were acquired in the presence of different fragments at the same pH as for crystallography *i.e.* pH~6.0. The experiments conducted on fragments **3** and **5**, indicate that the change in pH does not preclude compound binding for these 2 fragments. These compounds were submitted to X-ray crystallography but exhibited weak diffraction *i.e.* higher than 7 Å.

The lack of crystal structures of compounds from the TINS screen, in addition to the odd behavior of the compounds in the biochemical assay, lead us to question the relevance of the TINS screen. In this chapter, SPR and [¹⁵N,¹H]-HSQC NMR were used to confirm interaction of the compounds with EphA4 KD. Moreover, compounds **7** and

44, each originating from a different TINS screen, were shown to bind to the ATP binding site. The similarity of the structure of compound **7** and **27** suggests that the same compounds found computationally have also been found experimentally, a reassuring and exciting result.